

Structure and Electric Conductivity of Mixed Electronic–Ionic $\text{Bi}_2\text{O}_3\text{-Li}_2\text{O-V}_2\text{O}_5\text{-B}_2\text{O}_3$ Glass System

M. Shapaan*

Physics Department, Faculty of Science, Al-Azhar University, Nasr City, Cairo 11884, Egypt.

Received: 21 Sep. 2016, Revised: 22 Dec. 2016, Accepted: 24 Dec. 2016.

Published online: 1 Jan. 2017.

Abstract: In the present study, semiconducting glasses with composition $x\text{Bi}_2\text{O}_3\text{-(}20\text{-}x\text{)Li}_2\text{O-}20\text{V}_2\text{O}_5\text{-}60\text{B}_2\text{O}_3$ ($0 \leq x \leq 15$) mol % have been prepared by the conventional melt quenching technique. The glassy state of the as prepared samples is characterized using X-ray diffraction (XRD). The density and molar volume of the investigated glass system increase with increasing Bi_2O_3 content. The infrared spectra of these glasses are recorded over a continuous spectral range ($400\text{-}4000\text{ cm}^{-1}$) as an attempt to study their structure systematically. FT-IR spectroscopy data reveal that B_2O_3 and Bi_2O_3 behave as network formers and incorporated in the vitreous network as $[\text{BO}_3]$, $[\text{BO}_4]$, $[\text{BiO}_3]$, $[\text{BiO}_6]$, also V_2O_5 incorporated in the vitreous network as $[\text{VO}_4]$ and $[\text{VO}_5]$ structural units. Also it is found that the number of non-bridging oxygen ions (NBOs) increases with increasing Bi_2O_3 content. The measured DC conductivity, σ_{dc} , increases and the activation energy decreases at low temperature region at the same time the conductivity at high temperature region decreases and the activation energy increases with increasing Bi_2O_3 content. DC conductivity at room temperature (303 K) is typically $10^{-7}\text{-}10^{-6}$ ($\Omega^{-1}\text{m}^{-1}$) with activation energies at low and high temperature regions 0.34-0.17 (eV) and 0.80-0.64 (eV) respectively. Debye temperature, θ_D , increases with increasing Bi_2O_3 content with typical values 768-860 K.

Keywords: Oxide glasses; Density; IR spectroscopy; DC conductivity

1 Introduction

The semiconducting oxide glasses containing heavy metal oxide (HMO) such as bismuth oxide (Bi_2O_3) have received increased interest because of their possible applications in the field of glass ceramics, layers for optical and optoelectronic devices, thermal and mechanical sensors and reflecting windows [1-4]. Also borate glasses containing unconventional Bi_2O_3 as network former possess high refractive index, high optical basicity, extended far IR transmission and high non-linear optical susceptibility [3-5]. The interest for the investigated glassy system is determined by the presence of two network forming oxides, the classical B_2O_3 and unconventional Bi_2O_3 in addition to the presence of transition metal oxide (TMO) V_2O_5 and alkali oxide Li_2O . It was known that B_2O_3 is one of the most common glass formers. According to Krogh-Moe [6] the structure of vitreous B_2O_3 consists of a random network of boroxol rings and $[\text{BO}_3]$ triangles connected by B-O-B linkages. At the same time Bi_2O_3 may build a glass network of $[\text{BiO}_3]$ and $[\text{BiO}_6]$ polyhedra over a wide compositional range [7, 8]. An important class of glasses is the one which containing transition metal oxides (TMOs) such as V_2O_5 which exhibit semiconducting properties due to the existence of transition metal ions (TMIs) in more than one valence state (V^{4+} and

V^{5+}) [9, 10]. The electron-phonon interaction in these glasses is strong enough to form small polaron, and the electrical conduction process occurs by the hopping of small polarons between different valence states as proposed by Austin and Mott [11]. Recent studies shown that the electric conduction in glasses containing V_2O_5 (TMOs) may be attributed to small polarons hopping (SPH) which occurs from the low valence states (V^{4+}) to the neighboring high valence states (V^{5+}) [12-16]. The present work has been carried out to study the effect of partial replacement of Li_2O by Bi_2O_3 on the structure and electric conduction of the as prepared semiconducting glass samples of composition $x\text{Bi}_2\text{O}_3\text{-(}20\text{-}x\text{)Li}_2\text{O-}20\text{V}_2\text{O}_5\text{-}60\text{B}_2\text{O}_3$ ($0 \leq x \leq 15$) mol %.

2 Experimental Procedures

2.1 Sample Preparation and density measurement

The semiconducting glass system having the general chemical formula $x\text{Bi}_2\text{O}_3\text{-(}20\text{-}x\text{)Li}_2\text{O-}20\text{V}_2\text{O}_5\text{-}60\text{B}_2\text{O}_3$ ($x = 0, 5, 10, \text{ and } 15$ mol %) have been prepared by the melt quenching technique. The preparation is carried out by melting homogeneous mixtures of reagent grade H_3BO_3 , V_2O_5 , Bi_2O_3 and Li_2CO_3 (with purity not less than 99.8 %)

*Corresponding author E-mail: shapaan100@yahoo.com

in porcelain crucibles using an electric furnace at 1000 °C for 2 h. The melts are quenched between two pre-cooled copper plates to form (2cmx2cmx2mm) glass samples.

The glassy states of the as-prepared samples of the investigated system are detected using a Philips X-ray diffractometer PW/1710 with Ni filtered, Cu K α radiation ($\lambda = 1.542 \text{ \AA}$) powered at 40 (kV) and 30 (mA) (Figure 1). The room temperature densities, ρ , of the as prepared glass samples are measured using the suspension weight method based on Archimedes principle using toluene as an immersion liquid whose density is (0.868 g/cm 3).

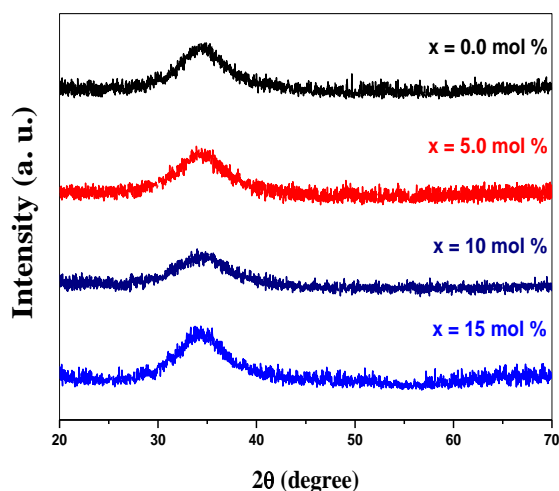


Fig. 1. XRD patterns for the as prepared $x\text{Bi}_2\text{O}_3$ -(20-x) Li_2O -20 V_2O_5 -60 B_2O_3 ($x = 0, 5, 10$ and 15 mol \%) system.

2.2 FT-IR measurements

In order to investigate the local order characterizing vitreous materials Fourier transform infrared (FT-IR) spectroscopy is a very sensitive and one of the most used spectroscopic methods. The infrared (IR) absorption spectra of the glasses in the wavenumber range (from 4000 to 400 cm^{-1}) with a resolution of 4 cm^{-1} are measured at room temperature by an infrared spectrophotometer type JASCO, FT/IR-430 (Japan).

2.3 DC conductivity measurements

The DC conductivity, σ_{dc} , of the as-quenched glasses is measured at temperatures between 300 and 600 K and under a constant DC voltage. For electric measurements the as prepared glass samples are polished to obtain optically parallel surfaces of 1.5 (mm) thickness. In order to achieve the best electrical contact between the glass samples and the electrodes of the sample holder the measurements are carried out on the silver paste coated pellets. The value of the current at different temperatures is measured using a Picoammeter (Keithley 485 Autoranging Picoammeter) and the I - V characteristic between electrodes is verified.

3 Results and Discussion

3.1 Density and molar volume

The variation in the density with composition in oxide glass system can be expressed in terms of apparent volume occupied by 1g atom of oxygen (molar volume V_m) which can be calculated from the density and composition using the following formula [17];

$$V_m = \sum(n_i M_w) / \rho \quad (1)$$

where, M_w , is the molecular weight of oxide, n_i , is the molar fraction and, ρ , is the density of the sample. Fig. 2a shows the variation of the measured room temperature density, ρ , of the as prepared $x\text{Bi}_2\text{O}_3$ -(20-x) Li_2O -20 V_2O_5 -60 B_2O_3 ($x = 0, 5, 10$ and 15 mol \%) glass samples. Fig. 2b shows the variation of the molar volume, V_m , of the investigated glassy system as a function of Bi_2O_3 content. The relative error in the density measurements is about $\pm 0.01 \text{ (g/cm}^3\text{)}$. It is found that the density and molar volume increase with increasing Bi_2O_3 content. This may be due to the higher molecular weight of Bi_2O_3 when compared to Li_2O .

This is not the general behavior which may expect for the density and molar volume. Where the general behavior should show opposite behavior to each other, but in the investigated glasses the behavior is different. This behavior may be attributed to that, the rate of increasing in molecular weight, M_w , is greater than the rate of increasing in density, ρ , (eq. 1). The same behavior for, ρ , and, V_m , was found earlier for many semiconducting glass systems containing Bi_2O_3 [17-21].

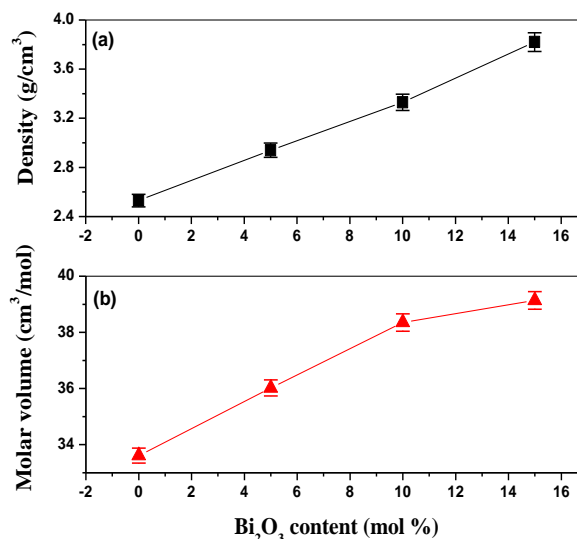


Fig. 2. Density and molar volume of the $x\text{Bi}_2\text{O}_3$ -(20-x) Li_2O -20 V_2O_5 -60 B_2O_3 ($x = 0, 5, 10$ and 15 mol \%) glass samples as a function of Bi_2O_3 content.

3.2 Infrared spectral studies

Table 1. Deconvolution parameters of the infrared spectra of $x\text{Bi}_2\text{O}_3\text{-(20-x)Li}_2\text{O-20V}_2\text{O}_5\text{-60B}_2\text{O}_3$ ($x = 0, 5, 10$ and 15 mol %) glasses. C is the component band center and A is the relative area (%) of the component band.

x = 0		x = 5		x = 10		x = 15		Assignments
C	A	C	A	C	A	C	A	
443	1.3	448	1.3	455	49.4	459	7.3	443 : Vibrations of angular deformation vibration of the O-V bond.
510	4.6	521	6.8	532	35.4	541	8.5	448-459 : Bi-O bend in BiO_6 units, vibrations of angular deformation vibration of the O-V bond.
632	6.2	637	10.8	642	19.4	686	12.3	510 : Bending vibration of BO_3 units.
700	6.7	702	11.3	702	23.5	700	13.7	521-541 : Bi-O bend in BiO_6 units, bending vibration of BO_3 units.
793	9.7	803	14.8	834	24.9	864	17.3	632-686 : antisymmetric vibrational modes of V-O-V group.
952	14.2	957	23.8	974	30.8	996	8.4	700-702 : Bending vibration of B-O-B in BO_3 triangles, antisymmetric vibrational modes of V-O-V group.
1129	10.3	1118	15.2	1108	33.7	1099	5.4	793 : B-O bond stretching of tetrahedral BO_4 units.
1252	4.9	1244	7.4	1235	19.8	1228	7.5	803-864 : B-O bond stretching of tetrahedral BO_4 units, Bi-O bond in the BiO_3 polyhedra.
1327	5.0	1327	12.8	1322	17.7	1320	7.3	952 : B-O stretch in BO_4 units from diborate groups Symmetric stretching vibrations of the isolated VO_2 group in VO_4 polyhedra, V=O band of VO_5 group.
1407	5.6	1399	11.3	1387	28.5	1383	8.3	957-996 : B-O stretch in BO_4 units from diborate groups, Bi-O bond in the BiO_3 polyhedra, Symmetric stretching vibrations of the isolated VO_2 group in VO_4 polyhedra V=O band of VO_5 group.
1516	11.7	1504	14.9	1464	14.6	1437	7.1	1129-1099 : Tetrahedral BO_4 borate units.
1526	15.3	1520	13.6	1515	2.7	1510	2.3	1200-1600 cm^{-1} : Stretching vibration of B-O-B in BO_3 triangles only.

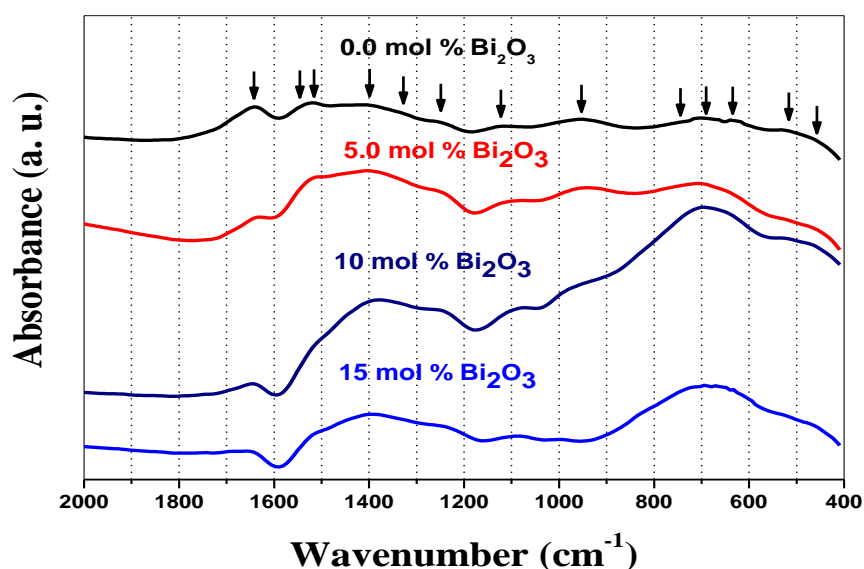


Fig. 3. Infrared absorption spectra of the $x\text{Bi}_2\text{O}_3\text{-(20-x)Li}_2\text{O-20V}_2\text{O}_5\text{-60B}_2\text{O}_3$ ($x = 0, 5, 10$ and 15 mol %) glass samples.

The obtained IR spectra of all the investigated glass samples are shown in Fig. 3, and the de-convolution analysis method is used to inspect the obtained IR bands where many different bands are clearly observed. These bands indicated the presence of different structural units in the glass network. Fig. 4 shows the de-convolution analysis for the IR spectra of the glass samples containing 0 and 15 mol % Bi_2O_3 , as representative curves. As shown in this Figure, the result of peak de-convolution indicates a

number of 13 peaks in the spectral range from 400 to 1650 cm^{-1} . Each individual band has its characteristic parameters such as its center (C), which is related to some type of vibration of a specific structural group, and its relative area (A), which is proportional to the concentration of that structural group. The de-convolution parameters, the band center (C) and the relative area (A) as well as the band assignment are given in Table 1. The bands around ~ 1640 cm^{-1} for all the investigated glass samples are assigned to

crystal water with H-O-H bending mode. For the Bi_2O_3 free glass sample ($x = 0$ mol %) the FT-IR spectrum of vitreous glass matrix contain three major absorption bands in the wavenumber ranges of $400\text{--}800\text{ cm}^{-1}$, $800\text{--}1200\text{ cm}^{-1}$ and $1200\text{--}1600\text{ cm}^{-1}$. In the first wavenumber region $400\text{--}800\text{ cm}^{-1}$ five absorption bands are observed, at $\sim 443\text{ cm}^{-1}$ may be attributed to vibrations of angular deformation vibration of the O-V bond, the band around $\sim 510\text{ cm}^{-1}$ can be attributed to the borate deformation modes, such as the in-plane bending of boron-oxygen triangles [22], at $\sim 632\text{--}686\text{ cm}^{-1}$ were assigned to the anti-symmetric vibrational modes of V-O-V group, at $\sim 700\text{--}702\text{ cm}^{-1}$ that were assigned to combination of the bending vibration of B-O-B in BO_3 triangles and anti-symmetric vibrational modes of V-O-V group [23-25] and at ~ 793 which was assigned to the B-O bond stretching of tetrahedral BO_4 units [26-30].

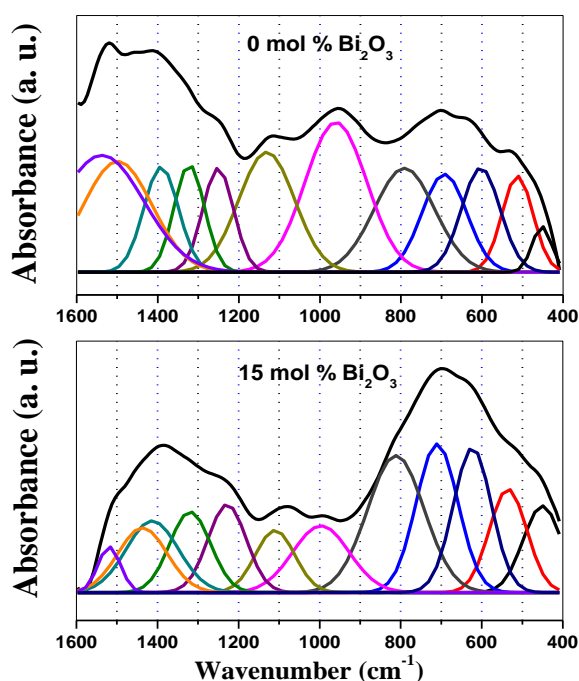


Fig. 4. Band deconvolution of IR spectra of the $x\text{Bi}_2\text{O}_3\text{--}(20-x)\text{Li}_2\text{O--}20\text{V}_2\text{O}_5\text{--}60\text{B}_2\text{O}_3$ ($x = 0$ and 15 mol %) glass samples.

The second wavenumber range, $800\text{--}1200\text{ cm}^{-1}$ contains two absorption bands at $\sim 952\text{ cm}^{-1}$ which are due to the combination of the B-O stretching bond in BO_4 units from diborate groups, symmetric stretching vibrations of the isolated VO_2 group in VO_4 polyhedra and V=O band of VO_5 group [24, 27, 31] as well as at $\sim 1129\text{--}1099\text{ cm}^{-1}$ which were assigned to tetrahedral BO_4 borate units. The third wavenumber range, $1200\text{--}1600\text{ cm}^{-1}$ contains five absorption bands at ~ 1252 , ~ 1327 , ~ 1407 , ~ 1516 and $\sim 1526\text{ cm}^{-1}$ which were assigned to stretching vibration of B-O-B in BO_3 triangles only [27-29]. From the FT-IR analysis it is found that the centers of the following absorption

bands at ~ 443 , ~ 510 , ~ 632 , ~ 793 and $\sim 952\text{ cm}^{-1}$ are shifted to higher wavenumbers and higher intensities for the glass sample $5\text{Bi}_2\text{O}_3\text{--}15\text{Li}_2\text{O--}20\text{V}_2\text{O}_5\text{--}60\text{B}_2\text{O}_3$ ($x = 5$ mol %). At the same time the following absorption bands at ~ 1129 , 1252 , 1327 , 1407 , 1516 and 1526 cm^{-1} are shifted to lower wavenumbers and higher intensities.

The same absorption bands are found for the glass sample $10\text{Bi}_2\text{O}_3\text{--}10\text{Li}_2\text{O--}20\text{V}_2\text{O}_5\text{--}60\text{B}_2\text{O}_3$ ($x = 10$ mol %) as well, where the absorption bands in the region $400\text{--}1000\text{ cm}^{-1}$ are shifted to higher wavenumbers with higher intensities and the bands in the region $\sim 1000\text{--}1600\text{ cm}^{-1}$ are shifted to lower wavenumbers with higher intensities, likewise the same behavior is found also for the glass sample with $x = 15$ mol % except for the bands at around ~ 952 , 1129 , 1516 and 1526 cm^{-1} which are shifted to lower wavenumbers with lower intensities.

The shift of the vibrational band towards the lower wavenumber is ascribed to the increase in the bond length of B-O bonds indicating the conversion of BO_3 polyhedral (bridging oxygen ions) to BO_4 tetrahedral unit (non-bridging oxygen ions). The increase in intensities of the vibrational bands with increasing Bi_2O_3 content suggests that, the non-bridging oxygens start appearing in the structure in larger number and may be form other borate groups. Also the increase in intensities of these bands may be results from some of the Bi^{3+} ions are occupying tetrahedral positions. The most important condition for the existence of BiO_3 polyhedra is the presence of a band at $\sim 834\text{ cm}^{-1}$ in the FT-IR spectrum [3] for the glass sample with 10 mol % Bi_2O_3 . This means that, the absorption band at about $\sim 834\text{ cm}^{-1}$ is a combination of BiO_3 polyhedral and BO_4 tetrahedral units. This band is shifted to higher wavenumber ($\sim 864\text{ cm}^{-1}$) for the glass sample with 15 mol % Bi_2O_3 .

For the glass samples containing 5 , 10 and 15 mol % the bands from $448\text{--}459\text{ cm}^{-1}$ were assigned to the Bi-O bond vibrations in distorted BiO_6 octahedra units in addition to vibrations of angular deformation vibration of the O-V bond [3, 32, 33]. The bands at around $\sim 521\text{--}541\text{ cm}^{-1}$ are the overlapping of the vibrations of the Bi-O bonds in the BiO_6 octahedral unit [33], with the bands of the in-plane bending vibration of BO_3 units [26, 28, 30]. The absorption bands around $\sim 957\text{--}996\text{ cm}^{-1}$ may be attributed to the overlapping of the B-O stretching band in BO_4 units from diborate groups, Bi-O bond in the BiO_3 polyhedra and symmetric stretching vibrations of the isolated VO_2 group in VO_4 polyhedra [34, 35].

Therefore, the FT-IR absorption spectra of the investigated glass system have evidenced that boron ions are incorporated as BO_3 and BO_4 units, a part of bismuth ions are incorporated in the glass network as BiO_3 pyramidal and BiO_6 octahedral units and a part of vanadium ions is incorporated in the glass network as VO_4 and VO_5 units.

3.3 DC conductivity measurements

The conductivity of the investigated semiconducting oxide glass system which containing TMIs (V^{4+} & V^{5+}) as well as alkaline ions (Li^+) and Bi^{3+} ions should be mixed i.e. electronic and ionic. The effect of temperature and the effect of the partial replacement of Li_2O by Bi_2O_3 on the DC conductivity of the glass composition $xBi_2O_3-(20-x)Li_2O-20V_2O_5-60B_2O_3$ ($0 \leq x \leq 15$) mol % are studied in more details. It is found that the DC conductivity of the investigated glass system obeys the well-known Arrhenius formula;

$$\sigma_{dc} = \sigma_0 \exp[-E_{dc}/k_B T] \quad (2)$$

where, E_{dc} , is the activation energy for conduction, σ_0 , is the pre-exponential factor, k_B , is the Boltzmann constant and T is the absolute temperature in K. Fig. 5 shows the plot $\ln\sigma_{dc}$ vs. $1000/T$ and it is found that the measured DC

conductivity, σ_{dc} , increases with increasing temperature. Also it is found that, the DC conductivity varied linearly against T^{-1} at two temperature regions. The first region is the low temperature region where ($T < \theta_D/2$) and the second region is the high temperature region where ($T > \theta_D/2$), indicating that, the conduction of the present system is mainly electronic in the low temperature region and mixed (electronic and ionic) in the high temperature region [36, 37] where, θ_D , is the Debye temperature. The electric conduction mechanism at the low temperature region depends mainly on the electron hopping from the lower valance states (V^{4+}) to the higher valance states (V^{5+}) of the vanadium ions [12-16]. The increases of the DC conductivity, σ_{dc} , with increasing temperature may be attributed to the increase of the thermally activated small polarons hopping (SPH) [38, 39]. The effect of the partial replacement of Li_2O by Bi_2O_3 is studied as well (Figure 5).

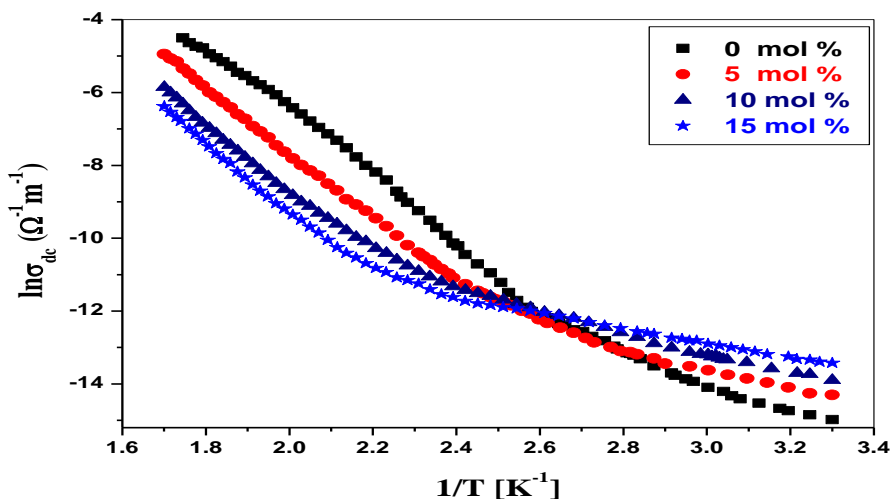


Fig. 5. The DC conductivity, σ_{dc} , of the $xBi_2O_3-(20-x)Li_2O-20V_2O_5-60B_2O_3$ ($x = 0, 5, 10$ and 15 mol %) glass samples as a function of reciprocal of temperature.

It is found that, at low temperature region the electric conductivity, σ_{dc} , increases with increasing Bi_2O_3 content [40]. The increases of the DC conductivity with the partial replacement of Li_2O by Bi_2O_3 at low temperature region ($T < \theta_D/2$) may be attributed to the increasing in the number of non-bridging oxygen ions (NBOs) and as a results increasing the open structure (i. e. the non-bridging oxygen ions) through which the charge carriers can move with higher mobility [41, 42]. These results are in a good agreement with the FT-IR results, where with increasing Bi_2O_3 content BO_3 polyhedral (bridging oxygen ions) convert to tetrahedral BO_4 (non-bridging oxygen ions). Virender Kundu et. al. reported that the formation of NBOs causes the decrease in band gap energy and as a result the DC conductivity increases with increasing Bi_2O_3 content [43]. At high temperature region where ($T > \theta_D/2$) both Bi^{3+} and Li^+ ions may become mobile and participate in the conduction process. It is found that the DC conductivity,

σ_{dc} , decreases with the partial replacement of Li_2O by Bi_2O_3 and this may be attributed to the lower mobility (higher ionic size) of Bi^{3+} ions compared to the higher mobility (lower ionic size) of Li^+ ions. In addition to that, with increasing Bi_2O_3 content new bonds of Bi-O-Bi and Bi-O-V may be formed that lead to decreasing the DC conductivity [44]. Fig. 6a and b show the variation of DC conductivity as a function of Bi_2O_3 content at different temperatures (303, 352, 442 and 518 K) as representative curves. The activation energies of the investigated glass samples are determined from the slope of $\ln\sigma_{dc}$ vs. $1000/T$. The activation energies are then evaluated by least square fitting method of eq. (2).

It is found that the activation energy (potential barrier) at the low temperature region decreases with increasing Bi_2O_3 content and at high temperature region it is found that the activation energy increases with increasing Bi_2O_3

content (Figure 7). The activation energies at low and high temperature regions are typically 0.34-0.17 eV and 0.64-0.80 eV respectively. Also it is found that Debye temperature, θ_D , increases with increasing Bi_2O_3 content (Figure 8) with typical values 768-860 K. Good agreement is found between the FT-IR results and the measured DC

conductivity. The values of the DC conductivity, σ_{dc} , at different temperatures (303, 352, 442 and 518 K) as an example, activation energies, E_{dc} , and Debye temperatures, θ_D , of the investigated glass samples are listed in Table 2.

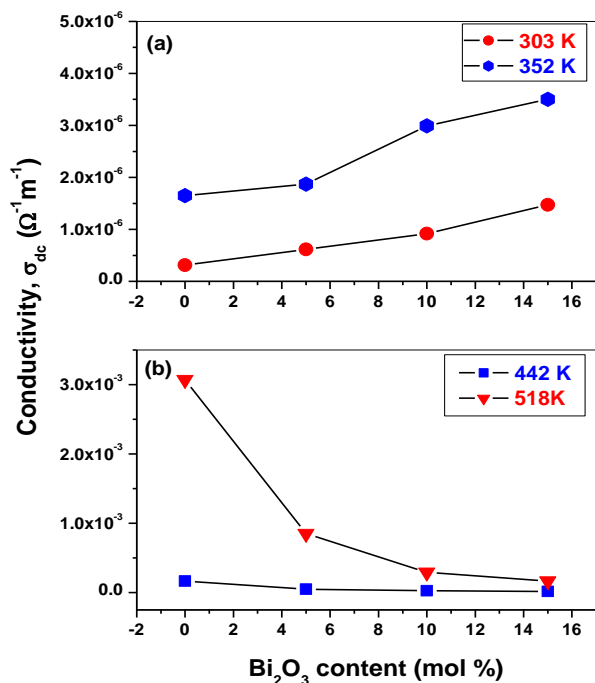


Fig. 6. DC conductivity of the investigated glass system as a function of Bi_2O_3 at different temperatures (303, 352, 442 and 518 K) as representative curves

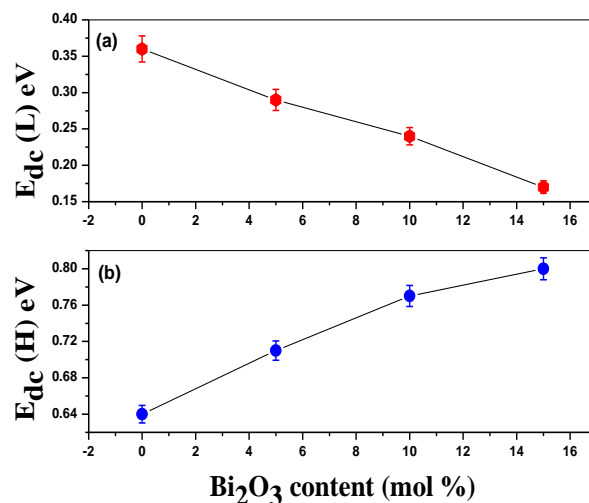


Fig. 7. The activation energies, $E_{dc}(L)$ and $E_{dc}(H)$ as a function of Bi_2O_3 content of the $x\text{Bi}_2\text{O}_3-(20-x)\text{Li}_2\text{O}-20\text{V}_2\text{O}_5-60\text{B}_2\text{O}_3$ ($x = 0, 5, 10$ and 15 mol %) glass samples.

Table 2. DC conductivity, σ_{dc} , at different temperatures (303, 352, 442 and 518 K), activation energy, E_{dc} , and Debye temperature, θ_D , of the $x\text{Bi}_2\text{O}_3-(20-x)\text{Li}_2\text{O}-20\text{V}_2\text{O}_5-60\text{B}_2\text{O}_3$ glass samples with ($x = 0, 5, 10$ and 15 mol %).

Bi_2O_3 mol %	σ_{dc} ($\Omega^{-1} \text{m}^{-1}$)	σ_{dc} ($\Omega^{-1} \text{m}^{-1}$)	σ_{dc} ($\Omega^{-1} \text{m}^{-1}$)	σ_{dc} ($\Omega^{-1} \text{m}^{-1}$)	E_{dc} (L)	E_{dc} (H)	$(\theta_D/2)$
	303 K	352 K	442 K	518 K	eV	eV	± 2 K
0	3.12×10^{-7}	1.65×10^{-6}	1.64×10^{-4}	3.07×10^{-3}	0.34 ± 0.09	0.64 ± 0.08	384
5	6.16×10^{-7}	1.87×10^{-6}	4.87×10^{-5}	8.5×10^{-4}	0.29 ± 0.04	0.71 ± 0.09	405
10	9.18×10^{-7}	2.99×10^{-6}	2.49×10^{-5}	2.92×10^{-4}	0.24 ± 0.05	0.77 ± 0.06	416
15	1.47×10^{-6}	3.5×10^{-6}	1.54×10^{-5}	1.66×10^{-4}	0.17 ± 0.01	0.80 ± 0.04	430

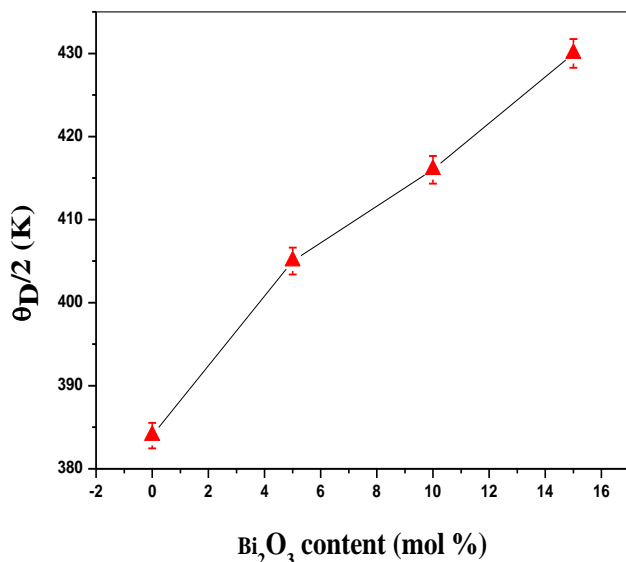


Fig. 8. Debye temperature, θ_D , as a function of Bi_2O_3 content of the $x\text{Bi}_2\text{O}_3-(20-x)\text{Li}_2\text{O}-20\text{V}_2\text{O}_5-60\text{B}_2\text{O}_3$ ($x = 0, 5, 10$ and 15 mol %) glass samples.

4 Conclusions

The structure and electric conduction of the semiconducting glass system with composition $x\text{Bi}_2\text{O}_3-(20-x)\text{Li}_2\text{O}-20\text{V}_2\text{O}_5-60\text{B}_2\text{O}_3$ ($0 \leq x \leq 15$) mol % are studied in more details.

It is found that the density and molar volume increases with increasing Bi_2O_3 content.

The FT-IR absorption spectra of the investigated glass system have evidenced that boron ions are incorporated as BO_3 and BO_4 units and a part of bismuth ions are incorporated in the glass network as BiO_3 pyramidal and BiO_6 octahedral units as well as a part of vanadium ions is incorporated in the glass network as VO_4 and VO_5 units. With increasing Bi_2O_3 the BO_3 (bridging oxygen ions) converted to BO_4 (non-bridging oxygen ions) tetrahedral.

The DC conductivity varied linearly against the reciprocal of temperature at two temperature regions and these observations suggest that the glasses under study show mixed conductivity i.e. electronic as well as ionic.

The Dc conductivity increases at the low temperature region (below Debye temperature) and decreases at high temperature region (above Debye temperature) with increasing Bi_2O_3 content. Debye temperature increases with increasing Bi_2O_3 content.

References

[1] S. Bale, N. Srinivasa Rao, S. Rahman, *Solid State Sci.* 10 (2008) 326.
 [2] S. Bale, M. Purnima, C.H. Srinivasu, S. Rahman, *J. Alloys & Compd.* 457 (2008) 545.

[3] V. Dimitrov, Y. Dimitriev, A. Montenero, *J. Non-Cryst. Solids* 51 (1994) 180.
 [4] D. Hall, N. Newhouse, N. Borrelli, W. Dumbaugh, D. Weidman, *J. Appl. Phys. Lett.* 54 (1998) 1293.
 [5] K. Knoblochova, H. Ticha, J. Schwarz, L. Tichy, *Optical Materials* 31 (2009) 895.
 [6] J. Krogh-Moe, *Phys. Chem. Glasses* 3 (1962) 101.
 [7] A. Pan, A. Ghosh, *J. Non-Cryst. Solids* 271 (2000) 157.
 [8] W.H. Dumbaugh, *Phys. Chem. Glasses* 27 (1986) 119.
 [9] Dhote DS, *Int. Res. J. of Science & Engineering* 2 (2014) 161.
 [10] N.F. Mott, *J. Non-Cryst. Solids* 1 (1968) 1.
 [11] I.G. Austin, N.F. Mott, *Advances in Physics* 18 (1969) 41.
 [12] L. Montagne, G. Palavit, G. Mairesse, *Phys. Chem. Glasses* 37 (1996) 206.
 [13] B. Santic, A. Mougis-Miliankovic, D.E. Day, *J. Non-Cryst. Solids* 296 (2001) 65.
 [14] M. Shapaan, E.R. Shabaan, A.G. Mostafa, *Physica B* 404 (2009) 2058.
 [15] M. Shapaan, *J. Non-Cryst. Solids* 356 (2010) 314.
 [16] M. Shapaan, *Int. J. New. Hor. Phys.* 3 (2016) 55.
 [17] Dorina Rusu, I. Ardelean, *Materials Research Bulletin* 43 (2008) 1724.
 [18] Y. Saddeek, A. Abousehly, S. Hussien, *J. Phys. D: Appl. Phys.* 40 (2007) 4674.
 [19] M.G. Moustafa, *Ceramics International* 42 (2016) 17723.
 [20] M. Shapaan, S.A. El-Badry, A.G. Mostafa, M.Y. Hassaan, M.H. Hazzaa, *J. Phys. Chem. Solids* 73 (2012) 4007.
 [21] A. Chahine, M. Et-tabirou, J.L. Pascal, *Materials Letters* 58 (2004) 2776.
 [22] E.I. Kamitsos, G.D. Chryssikos, *Solid State Ionics* 105 (1998) 75.
 [23] S. Mandal, S. Hazra, D. Das, A. Ghosh, *J. Non-Cryst. Solids* 183 (1995) 315.
 [24] M. Abo-Naf, F.H. El-Batal, M.A. Azooz, *Mater. Chem. Phys.* 77 (2002) 846.
 [25] A.K. Hassan, L. Borjesson, L.M. Torell, *J. Non-Cryst. Solids* 172 (1994) 154.
 [26] E.I. Kamitsos, A.P. Patsis, M.A. Karakassides, G.D. Chryssikos, *J. Non-Cryst. Solids* 52 (1990) 126.
 [27] Yasser B. Saddeek, M.S. Gaafar, *Materials Chemistry and Physics* 115 (2009) 280.
 [28] E.I. Kamitsos, M.A. Karakassides, G.D. Chryssikos, *J. Phys. Chem.* 91 (1987) 1073.
 [29] E.I. Kamitsos, M.A. Karakassides, G.D. Chryssikos, *Phys. Chem. Glasses* 28 (1987) 203.
 [30] Chryssikos G, Liu L, Varsamis C, Kamitsos E, *J. Non-Cryst. Solids* 235 (1998) 761.

- [31] S. Hayakawa, T. Yoko, S. Sakka, J. Ceram. Sot. Jpn. 102(1994) 522.
- [32] Hu Y, Liu NH, Lin UL, J. Mater. Sci. 229 (1998) 33.
- [33] L. Baia, R. Stefan, W. Kiefer, S. Simon, J. Raman Spectrosc. 36 (2005) 262.
- [34] K. Singh, Solid State Ionics 93 (1997) 147.
- [35] A. Bishay, C. Maghrabi, Phys. Chem. Glasses 10 (1969) 1.
- [36] A. Haouzi, M. Kharroubi, H. Belarbi, S. Devautour-Vinot, F. Henn, J.C. Giuntini, Applied Clay Science 27 (2004) 67.
- [37] H.H. Qiu, T. Ito, H. Sakata, Materials Chemistry and Physics 58 (1999) 243.
- [38] L. Murawski, R.J. Barczynski, Solid State Ionics 176 (2005) 2145.
- [39] S. Sindhu, S. Sanghi, A. Agarwal, Sonam, V.P. Seth, N. Kishore, Physica B 365 (2005) 65.
- [40] A.A. Ali, M.H. Shaaban, Physica B 403 (2008) 2461.
- [41] S. Rani, S. Sanghi, Anshu, A. Agarwal, N. Kishore, V.P. Seth, J. Physics and Chemistry of Solids 69 (2008) 1855.
- [42] B.V.R. Chowdari, Zhou Rong, Solid State Ionics 90 (1996) 151.
- [43] Virender Kundu, R.L. Dhiman, A.S. Maan, D.R. Goyal, S. Arora, J. Optoelectronic and Advanced Materials 12 (2010) 2373.
- [44] M. Shapaan, F.M. Ebrahim, Physica B 405 (2010) 3217.
-